

---

# Comparison and verification of tidal feature detection methods

---

## RESEARCH PROPOSAL



**UNSW**  
SYDNEY

---

Haotian Lyu | z5283856

Supervisor:  
Professor Sarah Brough

---

March 21, 2024

---

## 1 Background Theory

Our universe, or rather, the observable universe, contains stars, galaxies, and interstellar gas, as well as invisible dark matter and dark energy. The most accepted model of the universe is called the Lambda Cold Dark Matter ( $\Lambda$ CDM) Cosmological Model, the Lambda in its name ( $\Lambda$ ) is the cosmological constant driven by the dark energy and the dark matter is Cold Dark Matter. In this model, the formation of the structures in the universe such as galaxies and galaxy clusters follow the ‘hierarchical structure formation paradigm’ in that from the bottom up, the larger structures are formed through the continuous merging of smaller structures (Lacey & Cole, 1993). The ‘merger tree’ describing the evolution of a more massive structure is shown in Figure 1.

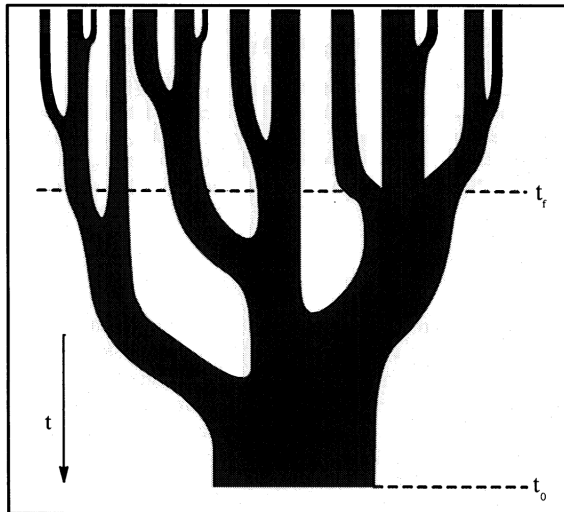


**Figure 1:** A schematic of a ‘merger tree’ that describes the growth of a massive structure as the result of a series of mergers. The widths of branches represent the masses of the structures, and time increases from top to bottom, where  $t_0$  is now and  $t_f$  is the time of formation of the final structures. Originally Figure.6 in Lacey & Cole (1993)

A key point for studying galaxy evolution is to study the mergers of galaxies. Although the hierarchical merger model is widely accepted qualitatively, there are still many details that need to be studied. This is particularly true for minor mergers, which are encounters where the secondary galaxy is less than 1/4 the mass of the primary galaxy. The contributions of minor mergers to galaxy evolution are very difficult to observe due to the faintness of the lower-mass galaxies. However, the hierarchical structure formation model indicates that low-mass collisions (minor mergers) play a significant role in the evolution of galaxies (e.g. Naab et al., 2009). Recent simulations from Martin et al. (2018) predict that most of the morphological evolution of galaxies since  $z \sim 1$  has been due to minor mergers.

There are several ways to observe and measure the mergers of galaxies, including detecting close pairs of galaxies that may merge in the future or detecting the tidal features left by galaxy mergers. Detecting close pairs uses spectroscopic observations to measure the distances to galaxies (e.g. Robotham et al. 2014). However, close pair detection has some limitations, for example, due to the potentially low mass of the secondary galaxies, spectroscopy may have difficulty detecting them (e.g. Lotz et al. 2011). In contrast, tidal feature detection does not have this limitation.

Tidal features are diffuse, non-uniform regions of stars that extend into space from galaxies and are formed by gravitational interactions between the galaxies. During the mergers of the galaxies, the gravitational force pulls out the stellar material into distinctive shapes. The examples of the main tidal feature morphologies are shown in Figure 2, including shells, stream, asymmetric halo, and double nucleus. The morphology, colour, and number of tidal features can offer important information about collisions and mergers. The number of tidal features indicates information about the rate of collisions, and the colour provides information on the mass of the parent galaxies involved in the collisions (Kado-Fong et al., 2018). Also, these features will exist for a few billion years after a collision and are still observable even if the secondary galaxies are low mass, making tidal feature detection a good method to investigate galaxy collisions over the last few billion years.

The research of tidal features faces difficulties due to the low surface brightness of the features, which can easily reach  $\mu_r \geq 27$  mag arcsec $^{-2}$  (Desmons et al., 2023). Such low surface brightness makes it difficult for wide-field optical astronomical surveys to detect these features. But such depth will be able to be reached in the next generation of wide-field optical imaging surveys, the Legacy Survey of Space and Time (LSST; Ivezić et al. 2019). This will be started in late-2025 by the Vera C. Rubin Observatory and will reach depths of  $\mu_r \sim 30.3$  mag arcsec $^{-2}$  (Martin et al., 2022).

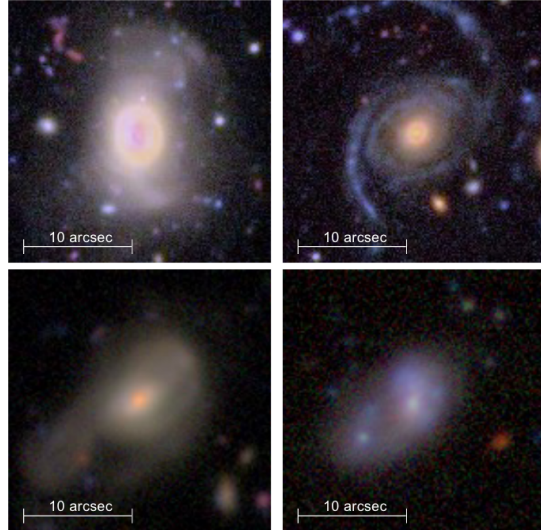


**Figure 2:** Example galaxies with different tidal feature morphologies. Top row from left to right: shells, stream. Bottom row from left to right: asymmetric halo, and double nucleus. Originally Figure.1 in Desmons et al. (2023)

With the commencement of LSST, a vast amount of images will be observed, predicted to detect billions of galaxies (Ivezić et al., 2019). The ensuing challenge is how to process this wealth of data. Previously, the identification, classification, and processing of tidal data relied primarily on visual identification by humans (e.g. Atkinson et al. 2013), which is clearly impractical for such a large volume of data. To solve this problem, Professor Sarah Brough and her team have begun developing methods that utilize Self-Supervised Representation Learning to automatically identify and extract galaxies with tidal features (Desmons et al., 2023). However, due to the lack of existing data on tidal features, this method requires further comparison and verification to better adapt to the upcoming massive LSST survey.

Cosmological hydrodynamical simulations are ideal laboratories to explore the physical mechanisms that form tidal features. Through these simulations, we have been able to delve more deeply into the merger histories of galaxies and understand the causes and differences in the formation of various types of tidal features. For example, simulations have shown that tail-like structures generally form from the mergers of galaxies with similar masses, also known as major mergers. In contrast, stream-like tidal features are often due to the infall of lower-mass satellite galaxies (minor mergers) (e.g. Hendel & Johnston 2015, Karademir et al. 2019). The formation of shells is subject to various theories, among which the most supported by observations and simulations is that shells are primarily formed through more radial mergers compared to tails and streams (e.g. Karademir et al. 2019). In the Illustris simulations by Pop et al. (2018), they found that the majority of the  $z \sim 0$  shells were produced by major mergers. For low-mass satellite galaxies (minor mergers), an almost purely radial infall was required to form shells.

An automated method for exploring galaxy mergers is the use of CAS (concentration, asymmetry, smoothness) parameters, which are a non-parametric method for measuring the forms of galaxies on resolved CCD images (Conselice et al., 2008). The CAS parameters are primarily based on the idea that the light distribution of galaxies provides insights into past and present formation modes (Conselice, 2003). The CAS parameters take a similar but independent approach to the method of detecting tidal features. A graphical representation of how CAS parameters are measured is given in Figure 3.

The asymmetry parameter A measures how symmetric a galaxy is, typically determined by taking an original image of the galaxy, rotating it 180 degrees about the galaxy's centre, and then subtracting the rotated image from the original image. The centre of the galaxy is identified by finding the point where the asymmetry is minimized. The formula of asymmetry A ([Conselice et al., 2008](#)) is given by:

$$A = \min \left( \frac{\sum |I_0 - I_{180}|}{\sum |I_0|} \right) - \min \left( \frac{\sum |B_0 - B_{180}|}{\sum |B_0|} \right) \quad (1)$$

where  $I_0$  is the original image and the  $I_{180}$  is the rotated image by 180 degrees. The second term is the correction for the background, where  $B_0$  is the light from a blank sky area and the  $B_{180}$  is the rotated version of  $B_0$ . The correction term is minimized in the same way as the original galaxy itself.

The smoothness (sometimes called clumpiness) parameter S measures the fraction of light in a galaxy that is contained in clumpy light concentrations. Clumpy structures have a significant amount of light at high spatial frequencies, while smooth systems, such as elliptical galaxies, have their light mainly at low spatial frequencies. The most common method to calculate the smoothness is described by [Conselice et al. \(2008\)](#) as follows:

$$S = 10 \left\{ \left( \frac{\sum (I_{x,y} - I_{x,y}^\sigma)}{\sum I_{x,y}} \right) - \left( \frac{\sum (B_{x,y} - B_{x,y}^\sigma)}{\sum I_{x,y}} \right) \right\} \quad (2)$$

where  $I_{x,y}$  is the original image's light intensity at position  $(x, y)$ , and  $I_{x,y}^\sigma$  is produced by blurring the original images with smoothing filter of size  $\sigma$ . Similar to the calculation of asymmetry, S have the correction for background, using the same smoothing kernel  $\sigma$  to blur the background intensity  $B_{x,y}$  to get  $B_{x,y}^\sigma$ . The smoothing kernel  $\sigma$  is determined by the radius of the galaxies that  $\sigma = 0.2 \times 1.5r(\eta = 0.2)$  ([Conselice, 2003](#)).

Concentration C is a parameter that measures how light is concentrated in a galaxy. It is typically measured using the ratio of the radii of two circular areas, which respectively contain 20% and 80% of the total light flux of the galaxy. The measurement of concentration C is:

$$C = 5 \log \left( \frac{r_{80}}{r_{20}} \right). \quad (3)$$

where  $r_{80}$  is the radius of the circular area that contains 80% of the total flux of the galaxy and  $r_{20}$  is the radius of the circular area that contains 20% of the total flux.

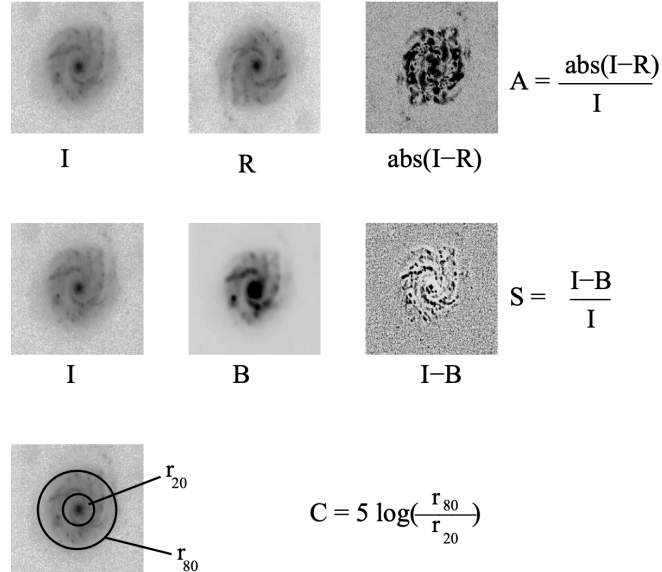


**Figure 3:** Graphical representation of how the CAS (asymmetry (A), clumpiness (S), and concentration (C)) parameters are measured. I is the original galaxy image, R is this image rotated by 180 degrees, and B is the image after it has been smoothed (blurred). Original Figure 3 in [Conselice \(2003\)](#).

Using CAS parameters, we can measure the morphology of galaxies and thus obtain information and mergers. For example, galaxies with  $A > 0.3$  are usually considered to be galaxies involved in mergers (Conselice et al., 2008). Figure 4 shows some example galaxy images with their values of asymmetry parameters.

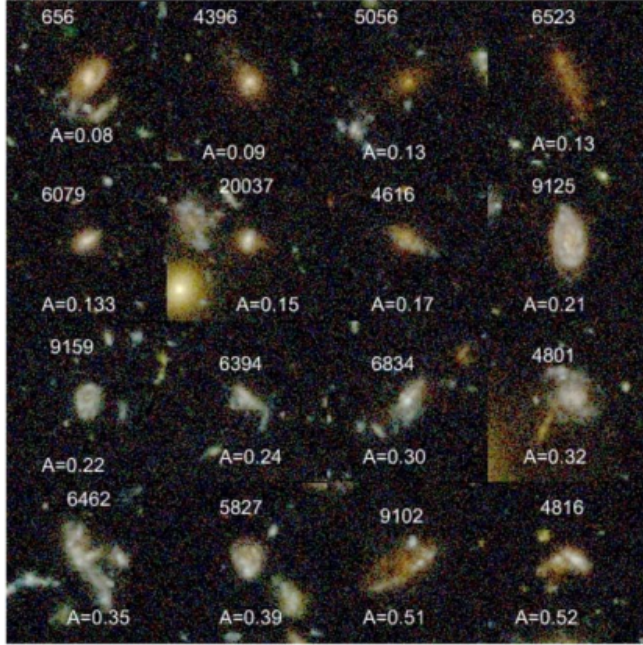


**Figure 4:** Example galaxy images with their corresponding asymmetry parameters. Plotted on the top of each image is the ID number from Coe et al. (2006), and the bottom number is the computed value of the asymmetry index in the B band. Original Figure 11 in Conselice et al. (2008).

## 2 Project Objectives

The primary aim of this project is to test the performance of automatic methods of identifying tidal features and to compare and validate these against other existing methods, in order to investigate the factors affecting the classification of tidal features. In this project, we will test Desmons et al. (2023)'s self-supervised representation learning algorithm on mock images of galaxies generated by cosmological simulations (Khalid et al. Subm) and compare the machine learning (ML) results with those from visual classification (Khalid et al. Subm). Through the similarities and differences between the visual and ML classification, we aim to gain a deeper understanding of the parameters in the algorithm that affect the classification of tidal features.

In addition to this, we will also explore where visually-identified and ML-identified tidal features sit in the CAS (concentration, asymmetry, smoothness) parameter space (Bershady et al., 2000). We will compare the CAS results with those of self-supervised learning methods and visual classification to assess the relationship of CAS parameters with the identification of tidal features. This will allow us to determine whether comparisons can be made between results obtained with these different approaches to finding galaxy mergers.

## 3 Project Motivations

Understanding the history of galaxy mergers and their evolution over time is crucial for studying galaxies and will provide a valuable test of the hydrodynamical formation model through simulations of that model. Tidal features provide an effective way to investigate the effect of galaxy mergers, which is essential for our understanding of galaxy evolution. At present, the studies and classification methods of tidal features are lacking and inefficient for the next generation of imaging surveys in the pipeline. Visual classification is becoming impossible for the upcoming flood of data, and there is an urgent need for sophisticated automatic classification algorithms to process the vast amount of data.

This Honours project aims to test the existing machine-learning algorithm for the automatic identification of tidal features. It will assess the effectiveness of the automatic classification on the mock images, and then compare the differences and similarities between the tidal features identified by ML and by visual classification. During the testing and comparison, we can explore the key features of recognizing tidal features, and then perfect the algorithms to prepare for the upcoming LSST data. The project will also investigate the relationship between tidal feature classifications and other automated methods of identifying galaxy mergers such as using the CAS parameters.

## 4 Data Sources And Models

The data for this Honours project will mainly be the mock images generated from Illustris hydro-dynamical cosmological simulations. The model that will be used in this project is the machine learning model developed by [Desmons et al. \(2023\)](#). We will develop our own code to measure CAS parameters on the mock images.

### 4.1 Mock images

We will use mock images from cosmological simulations to test the classification of the machine-learning algorithm from [Desmons et al. \(2023\)](#). The mock images of 1826 galaxies have already been generated using the “IllustrisTNG” ([Springel et al., 2017](#)) cosmological simulations by [Khalid et al. \(Subm\)](#). Example mock images are shown in Figure 5. These galaxies have different stellar masses  $M_*$  ranging from  $3.16 \times 10^9 M_\odot$  to  $6.50 \times 10^{11} M_\odot$ , with an average mass of  $2.67 \times 10^{10} M_\odot$ .

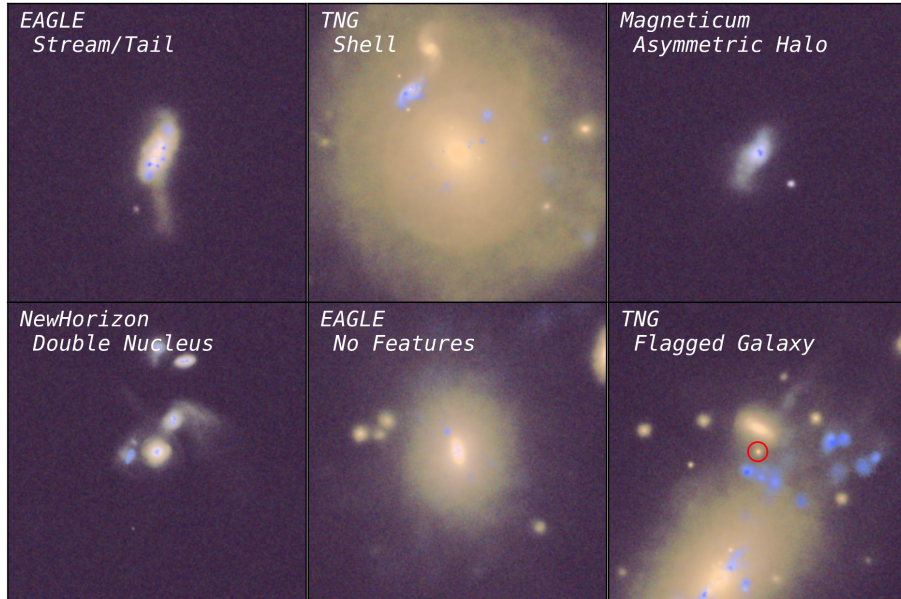


**Figure 5:** Examples of Mock images from different hierarchical cosmological simulations showing different tidal features. Original Figure 1 in [Khalid et al. \(Subm\)](#)

It is important to note that the mock images visually classified in [Khalid et al. \(Subm\)](#) and those that will be inputted into the self-supervised learning algorithm are different. In [Khalid et al. \(Subm\)](#), the mock images were placed close by, at a distance of  $z \sim 0.025$  (average  $\sim 105 Mpc$ ) to see all details. They are therefore sized 2400 pixels  $\times$  2400 pixels, as shown in Figure 5. However, the [Desmons et al. \(2023\)](#) model was developed for the Galaxy And Mass Assembly (GAMA; [Driver et al. 2011](#)) survey. This sample has a median distance of  $z \sim 0.2$ , so a cut-out of 128  $\times$  128 pixels was more appropriate. This is also more consistent with the types of images that LSST will provide. [Khalid et al. \(Subm\)](#) has re-made the mock images at a distance of  $z \sim 0.2$  with 128  $\times$  128 pixels. Figure 6 shows examples of the re-made mock images.

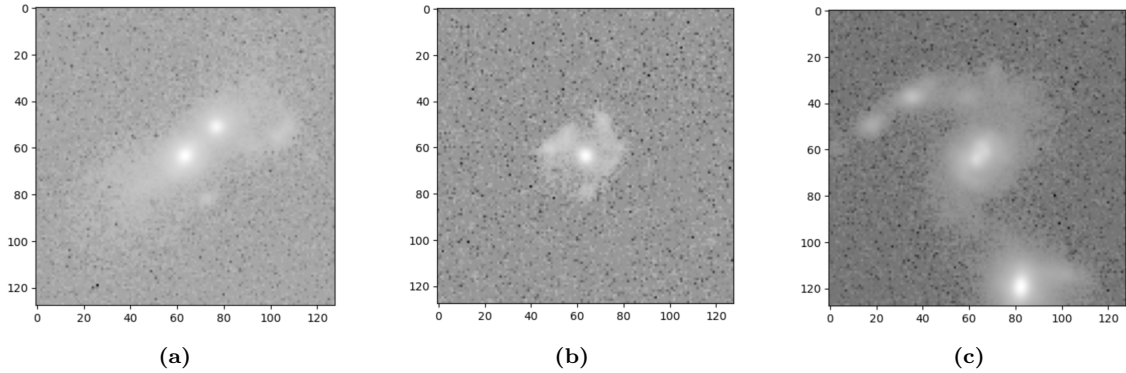


**Figure 6:** Examples of re-made mock images with tidal features. Figure 6a is classified as having a Double Nucleus (confidence level 2) and Halo (confidence 3), Figure 6b is classified as having a tail (confidence 2) and Halo (confidence 3), and Figure 6c is classified as having a tail (confidence 3). The confidence level with description can be seen in Table 1. Note that these visual classifications are based on the original mock images.

The mock images were visually classified by Khalid et al. (Subm) at their original distance. Table 1 shows the Confidence levels together with their corresponding descriptions.

Confidence Level	Description
0	No tidal feature detected.
1	Hint of tidal feature detected, classification difficult.
2	Even chance of correct classification of tidal feature presence and/or morphology.
3	High likelihood of the tidal feature being present and morphology being obvious.

**Table 1:** Descriptions of the classification confidence (Khalid et al. Subm.).

The data produced by hierarchical cosmological simulations ([Springel et al., 2017](#)) is stored in the UNSW supercomputer Katana. Katana is a shared computational cluster located on the UNSW campus, designed to provide access to computational resources for groups working with non-sensitive data ([Katana, 2024](#)).

## 4.2 Model Architecture

The machine learning model from Desmons et al. (2023) consists of two components: a self-supervised model used for pre-training, and a linear classifier used for classification.

#### 4.2.1 Self-Supervised Model

The self-supervised model uses a type of self-supervised learning called Nearest Neighbour Contrastive Learning of visual Representations (NNCLR; [Dwibedi et al. 2021](#)), Figure 7 shows the structure of the NNCLR used here.

Self-supervised learning models create various augmented versions of an image, then the model pairs images and categorizes them as positive or negative pairs. For instance, if  $x_i$  is the original image, for any pair  $(x_i, x_j)$ , if  $x_j$  is an augmented version of  $x_i$ , then the pair is labeled as a positive pair. Conversely, if  $x_j$  is not an augmented version of  $x_i$ , then it is a negative pair. For every image in the sample, the encoder networks in the model generate a 128-dimensional representation. This encoder is trained to produce similar representations for positive pairs and dissimilar representations for negative pairs, allowing for the clustering of similar samples while distancing dissimilar ones.

The encoder uses a contrastive loss function to create the representations for each image (Eqn. 4), but this contrastive learning has problems since it is based on the different augmented versions of the same image to create positive pairs, the objects with big differences but belong to the same class (such as galaxy with different tidal features) will not be linked.

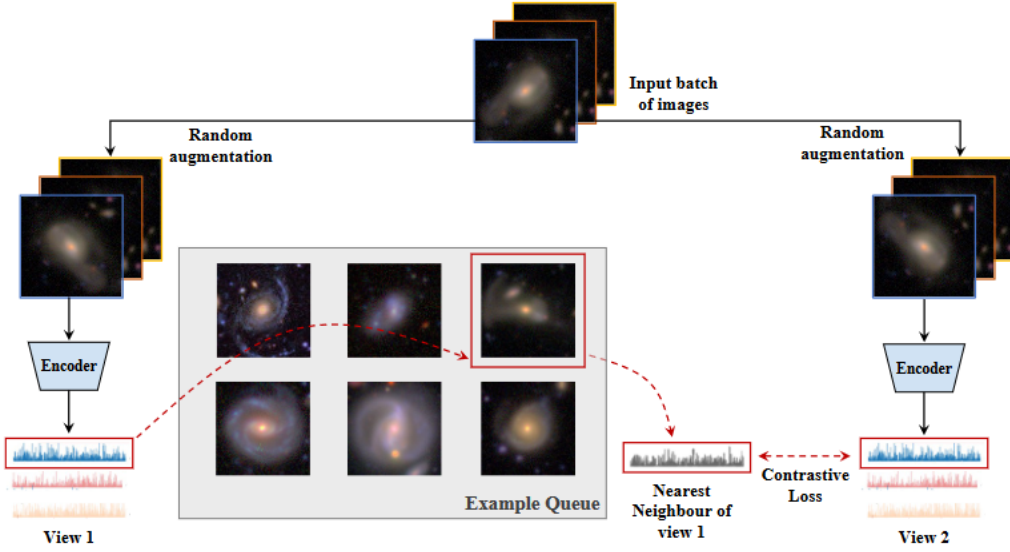


**Figure 7:** The schematic of Nearest Neighbour Contrastive Learning of Visual Representations. Original Figure 2 in [Desmons et al. \(2023\)](#)

$$L_i = -\log \left( \frac{\exp(\text{sim}(z_i, z_i^+))}{\exp(\text{sim}(z_i, z_i^+)) + \sum_{z^-} \exp(\text{sim}(z_i, z^-))} \right) \quad (4)$$

To address this problem, NNCLR does not simply create positive and negative pairs based on whether they are augmented versions of the original image. Instead, it creates a queue of samples and uses whether they are the nearest neighbors in the queue to define the positive and negative pairs for a given image. The contrastive loss function of NNCLR is:

$$L_i^{NNCLR} = -\log \left( \frac{\exp(\text{NN}(z_i, Q) \cdot z_i^+ / \tau)}{\sum_k \exp(\text{NN}(z_i, Q) \cdot z_k^+ / \tau)} \right) - \log \left( \frac{\exp(\text{NN}(z_k, Q) \cdot z_i^+ / \tau)}{\sum_k \exp(\text{NN}(z_k, Q) \cdot z_i^+ / \tau)} \right) \quad (5)$$

where  $Q$  is the queue of the sample and  $\text{NN}$  is the nearest neighbour operator that:

$$\text{NN}(z, Q) = \arg \min_{i \in Q} \|z - i\|_2 \quad (6)$$

where  $\|x\|_{l_2}$  is  $l_2$ -normalisation of  $x$ , which is:

$$\|x\|_2 = \sqrt{\sum_{k=1}^n |x_k|^2} \quad (7)$$

This model uses ResNet-50 as the encoder followed by a global pooling layer. After that, there are two 128-sized fully connected layers with L2 kernel regularisation and a penalty of 0.0005. A batch-normalisation layer follows each fully connected layer and ReLu activation follows the batch-normalisation layer ([Desmons et al., 2023](#)).

#### 4.2.2 The Linear Classifier

The training of the self-supervised model does not require labels for data, the encoder simply transforms images into meaningful low-dimensional representations based on their augmentations. However, since we need to classify galaxies based on tidal features, [Desmons et al. \(2023\)](#) has trained a linear classifier using a small dataset and the encoder to classify the images. The encoded representations from the Self Supervised Model are sent to a fully connected layer with a sigmoid activation, which outputs a single number between 0 and 1 to measure the likelihood of a single image having tidal features. We will compare the output of the linear classifier with the visual classification.

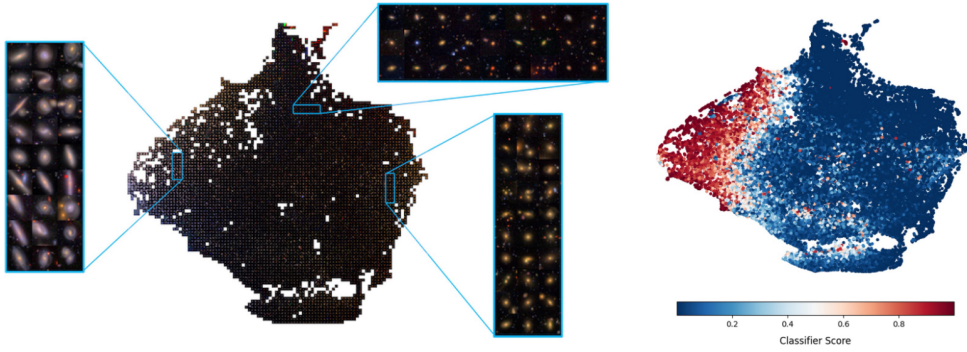


**Figure 8:** Left figure is the 2D Uniform Manifold Approximation and Projection (UMAP) projection of the representations from the self-supervised model. Made by binning the space into  $100 \times 100$  cells and randomly selecting a sample from that cell to plot in the corresponding cell location. The right figure is the same 2D UMAP projection without binning, coloured according to the scores assigned to each galaxy by the linear classifier. Original Figure 8 in [Desmons et al. \(2023\)](#)

## 5 Timeline

1. Obtain mock images from [Khalid et al. \(Subm\)](#).
2. Visually classify the re-made mock images ( $z \sim 0.2, 128 \times 128$  pixels), and compare the classification result with re-made mock images with that of the original mock images ( $z \sim 0.05, 2400 \times 2400$  pixels).
3. Convert mock images to the format required for input into the self-supervised machine learning modal ([Desmons et al., 2023](#)).
4. Input the mock images into the automatic classification algorithm to obtain machine learning classifications.
5. Compare the results of the visual classification of the mock images with those of the automatic classification algorithm to evaluate the capability of the automatic algorithm. Determine how this depends on the galaxy's properties like radius, brightness, or stellar mass. Perform parameter fine-tuning on the algorithm to test and improve its performance based on these findings.
6. Apply the CAS method to the mock images to assess its performance in the classification of tidal features. Determine where the visually-classified and ML-classified tidal features sit in the CAS parameters space. Through comparison, identify key factors that are critical in the detection of tidal features.

## 6 Preliminary Results

Step 1, has been completed. Since the data from the [Khalid et al. \(Subm\)](#) are in units of flux, we need to convert them into units of surface brightness (mag arcsec $^{-2}$ ) by using the equation:

$$\mu = -2.5 \log \frac{f}{\text{area}} \quad (8)$$

where the  $f$  is the flux, the area that of one pixel, which is  $0.4 \text{ arcsec}^{-2}$  ( $0.2'' \times 0.2''$ ), and  $\mu$  is the surface brightness in units of (mag arcsec $^{-2}$ ). Figure 6 is precisely the grayscale image converted from units of flux to units of surface brightness.

Step 2 is in progress. [Khalid et al. \(Subm\)](#) used the original images at a distance of  $z \sim 0.005$  with a resolution of  $2400 \times 2400$  pixels for the image classification. However, after re-making, the new images are at a distance of  $z \sim 0.2$  and only have a resolution of  $128 \times 128$  pixels, which makes many tidal features in the original images difficult to recognize in the re-made images. For example, in Figure 6b, [Khalid et al. \(Subm\)](#) classified the original image as having a tail (confidence level 2), but it is hard to see a tail in the re-made image. Since the images identified

by the self-supervised learning are the re-made images, it would be unreasonable to compare the original image classifications with the machine learning results obtained from the re-made images. Therefore, I need to visually reclassify the re-made images according to the classification standards shown in Table 1. I have now completed the classification of 50 re-made images. After checking and confirming the accuracy of these classifications with Professor Sarah Brough, I will continue to complete the classification of the remaining images.

Step 3: After confirming the input format for the self-supervised learning, the units of original mock images and the format required for self-supervised learning are the same, both in flux. However, the input images need to be normalized by dividing by  $3\sigma$ , where the  $\sigma$  is the standard deviation for each band (g, r, i, z y) of the image sample by using median absolute deviation, I need to calculate the standard deviation  $\sigma$  for mock images and normalize them before inputting them into the models.

Step 4: I already have access to the self-supervised model from GitHub ([Desmons & Lanusse, 2023](#)). Next, I need to understand the model and input the mock images.

## 7 Potential Complications

Typically, astronomical projects are influenced by complex weather conditions, for instance, astronomical observations require cloud-free skies for optimal viewing conditions. However, in this project, the only data used are mock images generated from hierarchical cosmological simulations, which are not affected by the complexities of weather.

Secondly, since it is necessary to use [Desmons et al. \(2023\)](#)'s self-supervised model, and this model has not had extensive testing in various versions of computer environments, there is a possibility that the model may not run properly due to different running environments. I will create an environment using Python 3.7.4, consistent with the model's environment ([Desmons & Lanusse, 2023](#)), to ensure the model operates as normally as possible.

Another potential complication is data loss. To avoid such issues, the data will be stored in multiple locations, such as locally, on GitHub, and on OneDrive, with timely updates and merges after any changes.

## References

- Atkinson A. M., Abraham R. G., Ferguson A. M. N., 2013, *The Astrophysical Journal*, 765, 28
- Bershady M. A., Jangren A., Conselice C. J., 2000, *The Astronomical Journal*, 119, 2645
- Coe D., Benítez N., Sánchez S. F., Jee M., Bouwens R., Ford H., 2006, *The Astronomical Journal*, 132, 926
- Conselice C. J., 2003, *The Astrophysical Journal Supplement Series*, 147, 1
- Conselice C. J., Rajgor S., Myers R., 2008, *Monthly Notices of the Royal Astronomical Society*, 386, 909
- Desmons A., Lanusse F., 2023, LSSTISSL/Tidalsaurus, <https://github.com/LSSTISSL/Tidalsaurus>
- Desmons A., Brough S., Lanusse F., 2023, Detecting Galaxy Tidal Features Using Self-Supervised Representation Learning ([arXiv:2308.07962](https://arxiv.org/abs/2308.07962))
- Driver S. P., et al., 2011, *Monthly Notices of the Royal Astronomical Society*, 413, 971
- Dwibedi D., Aytar Y., Tompson J., Sermanet P., Zisserman A., 2021, With a Little Help from My Friends: Nearest-Neighbor Contrastive Learning of Visual Representations, doi:10.48550/arXiv.2104.14548, <https://arxiv.org/abs/2104.14548>
- Hendel D., Johnston K. V., 2015, *Monthly Notices of the Royal Astronomical Society*, 454, 2472
- Ivezić Ž., et al., 2019, *The Astrophysical Journal*, 873, 111
- Kado-Fong E., et al., 2018, *The Astrophysical Journal*, 866, 103
- Karademir G. S., Remus R.-S., Burkert A., Dolag K., Hoffmann T. L., Moster B. P., Steinwandel U. P., Zhang J., 2019, *Monthly Notices of the Royal Astronomical Society*, 487, 318
- Katana 2024, Katana — UNSW Research, <https://research.unsw.edu.au/katana>
- Khalid A., Brough S., Martin G., Kimmig L., Subm, Characterising Tidal Features Around Galaxies in Cosmological Simulations
- Lacey C. G., Cole S., 1993, *Monthly Notices of the Royal Astronomical Society*, 262, 627
- Lotz J. M., Jonsson P., Cox T. J., Croton D., Primack J. R., Somerville R. S., Stewart K., 2011, *The Astrophysical Journal*, 742, 103
- Martin G., Kaviraj S., Devriendt J. E. G., Dubois Y., Pichon C., 2018, *Monthly Notices of the Royal Astronomical Society*, 480, 2266
- Martin G., et al., 2022, *Monthly Notices of the Royal Astronomical Society*, 513, 1459
- Naab T., Johansson P. H., Ostriker J. P., 2009, *The Astrophysical Journal*, 699, L178
- Pop A.-R., Pillepich A., Amorisco N. C., Hernquist L., 2018, *Monthly Notices of the Royal Astronomical Society*, 480, 1715
- Robotham A. S. G., et al., 2014, *Monthly Notices of the Royal Astronomical Society*, 444, 3986
- Springel V., et al., 2017, *Monthly Notices of the Royal Astronomical Society*, 475, 676